MISSOURI S&T

Missouri University of Science and Technology

Scholars' Mine

International Conferences on Recent Advances in Geotechnical Earthquake Engineering and Soil Dynamics

1991 - Second International Conference on Recent Advances in Geotechnical Earthquake Engineering & Soil Dynamics

12 Mar 1991, 2:30 pm - 3:30 pm

Soil Amplification Based on Array Observation in Chiba, Japan

Lin Lu
University of Tokyo, Japan

Tsuneo Katayama
University of Tokyo, Japan

Fumio Yamazaki
University of Tokyo, Japan

Follow this and additional works at: https://scholarsmine.mst.edu/icrageesd

🟡 Part of the Geotechnical Engineering Commons

Soil Amplification Based on Array Observation in Chiba, Japan

Jin Lu
Institute of Industrial Science, University of Tokyo, Tokyo, Japan

Tsuneo Katayama
Institute of Industrial Science, University of Tokyo, Tokyo, Japan

Fumio Yamazaki
Institute of Industrial Science, University of Tokyo, Tokyo, Japan

SYNOPSIS: The amplification characteristics of earthquake ground motion were investigated based on the Chiba Array observation records. The amplification of peak acceleration occurred mostly at the top soft layer and is similar for the three ground motion components. The ensemble Fourier spectrum ratio and coherence function were calculated and the amplification can be clearly seen in them. The drop of the coherence function at natural frequencies was discussed. The Fourier spectrum ratio and coherence function were also obtained using the smoothing procedure and were compared with those of the ensemble. Microtremor was measured at 11 points corresponding to the location of the surface accelerometers. The power spectrum of microtremor was compared with that of the earthquake ground motion for different points and for different events. Emphasis has been placed on knowing the property of the peaks appearing in the power spectra.

INTRODUCTION

Local site conditions can significantly influence the characteristics (amplitude, frequency contents and duration) of earthquake ground motions and hence influence the degree and extent of damage caused by an earthquake. The destruction of buildings in Mexico City (Bertero, 1986) due to the 1985 Michoacan earthquake and the structural damage (Benuska et al., 1990) in the San Francisco Bay Area due to the 1989 Loma Prieta earthquake are the typical examples providing further evidence of the fact that local soil conditions can have a major effect on both the nature of ground motion and on damage.

As the effect of local soil conditions comes mainly from the large amplification of ground motion at certain frequencies, investigation of soil amplification characteristics is extremely important. Soil amplification characteristics can provide information for the prediction of ground motion for a specific site and for the seismic safety assessment of existing structures. In this regard, soil amplification characteristics were investigated based on the Chiba array earthquake records. Because of the unique arrangement of seismometers in this array, the local effects of soil amplification within a small area were also examined.

Microtremor observation has been involved in earthquake engineering to evaluate site conditions (Kanai and Tanaka, 1961) and the characteristics of earthquake ground motion in microzoning (Sherif, 1981). Because of the difference of source, propagation pass and vibration amplitude between microtremor and earthquake ground motion, however, further investigation on microtremor is still necessary. The microtremor was measured in the Chiba experiment station at the locations of the surface (GL -1m)

accelerometers. The characteristics of microtremor were analyzed and were compared with those of earthquake ground motion.

CHIBA SEISMOMETER ARRAY AND ITS STRONG MOTION DATABASE

A three-dimensional array (Katayama and Sato, 1982) was established in 1982 at the Chiba Experiment Station of the Institute of Industrial Science, University of Tokyo. In the case of this array, the seismometers were buried at several depths in a total of 15 boreholes within an area of about 300m x 300m. The layout of the boreholes and the location
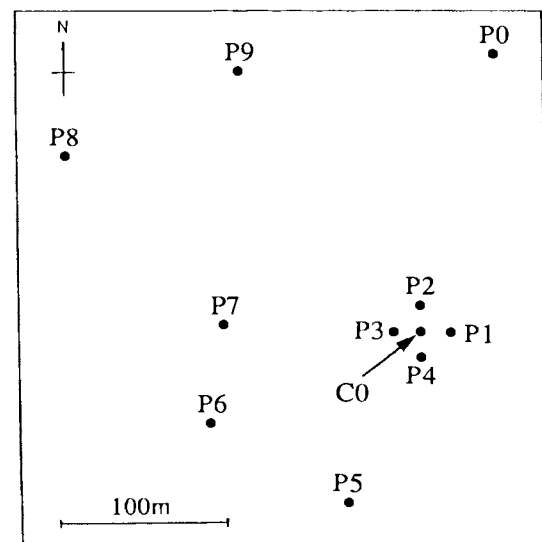

Fig. 1 Layout of Boreholes in Chiba Array

Table 1 Location of Borehole Accelerometers

Depth (m)	Borehole														
	CO	C1	C2	C3	C4	P1	P2	P3	P4	P5	P6	P7	P8	P9	PO
1	O	O	O	O	O	O	O	O	O	O	O	O	O	O	O
5	O	O	O	O	O										
1 0	O	O	O	O	O	O	O	O	O	O	O				
2 0	O					O	O	O	O	O	O	O	O	O	O
4 0	O										O				

borehole CO   borehole P5   borehole P6   borehole P7

Depth(m)	Borehole CO	
	P-wave(m/s)	S-wave(m/s)
0 - 5	320	140
5 - 15	550	320
15 - 24	1670	320
24 - 40	1670	420
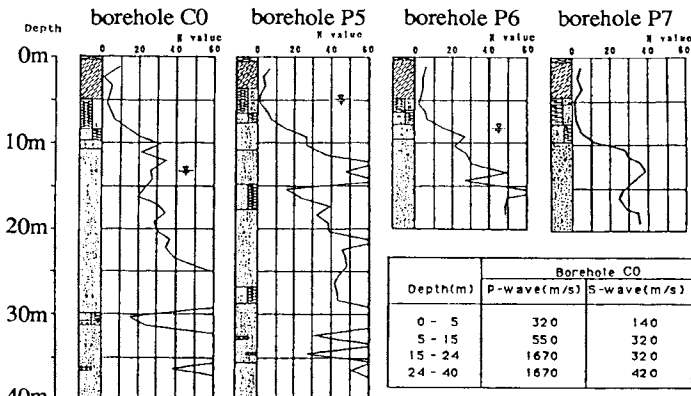
Fig. 2 Soil Profiles of Chiba Experiment Station

underlined earthquake
numbers for ensemble

70km radius from CHIBA

Fig. 3 Epicenters of Events in the Chiba Array Database

of the seismometers in each borehole are shown in Fig. 1 and Table 1 respectively. It should be noticed that boreholes C1 to C4, which are only 5m from borehole CO, are not marked in Fig. 1.

The Chiba Experiment Station is located about 30km east of Tokyo. The topographical and geological conditions of the array site are basically simple and the ground surface is almost flat. Figure 2 shows the soil profiles of the boreholes where the standard penetration tests were carried out. The top 3 - 5m of the site is covered with loam with a standard penetration N value of less than 10. The loam layer is underlain by a sandy clay layer of 2 - 4m in thickness having a N value of also less than 10. A diluvium sand layer lies under the clay layer and its N value is greater than 20 -30. This sand layer, the stiffness of which increases with depth, is interspersed with clayey layers with relatively small N values. In spite of the slight difference in the depths of boundaries between different layers from one borehole to another, the layering is quite uniform indicating a relative simple soil profile.

In borehole CO, the elastic wave velocities were measured by downhole shooting giving the results shown in Fig. 2. Although there are several low-storied buildings and research facilities in the Chiba Station, they are not so closely located to the boreholes. Thus the recorded ground motions can be considered free-field ones.

In the Chiba array, more than 160 earthquakes have been recorded since 1982. Because the trigger level is set relatively low, most of recorded events are small. Based on 27 major events whose peak ground acceleration at the ground surface is generally greater than 20cm/sec^2, a
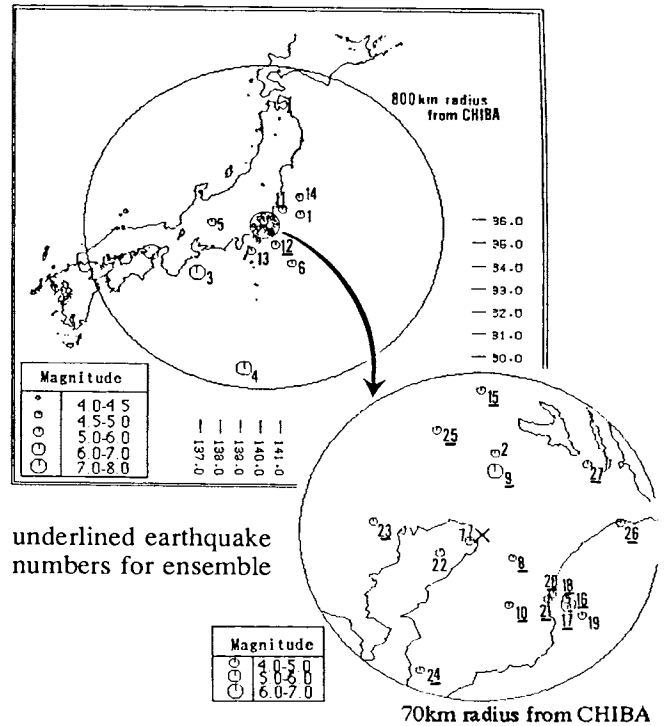
strong motion database (Nagata et al., 1990) has recently been created. The JMA magnitude of the events included in the database covers a range from 4.0 to 7.9 and the epicentral distance ranges from 5km and 702km as illustrated in Fig. 3. The largest peak acceleration at the ground surface is 327 cm/sec^2 due to the 1987 Chibaken-Toho-Oki earthquake (#16 in Fig. 3: event number IEQK = 8722). This database was employed in the present study to investigate the soil amplification characteristics.

SOIL AMPLIFICATION CHARACTERISTICS BASED ON EARTHQUAKE RECORDS

Peak Ground Acceleration

The amplification of peak acceleration was examined for borehole CO where ground motions were recorded at depths of 1, 5, 10, 20 and 40m from the ground surface. The recorded peak accelerations at GL -1, -5, -10 and -20m were normalized by those at GL -40m for the 27 events. The ratios for individual events are shown in Fig. 4 for the three components. Although the peak acceleration does not simply indicate the degree of structural damage due to the earthquake, the peak acceleration is commonly used to represent the intensity of ground motion.

The amplification mostly occurred at a level of a few meters below the ground surface and the amplification ratio was found to be rather similar for the three components. From the soil profile of borehole CO, it is known that the soil stiffness increases as the depth increases with the top 5m being much softer than the underlying layer. The peak
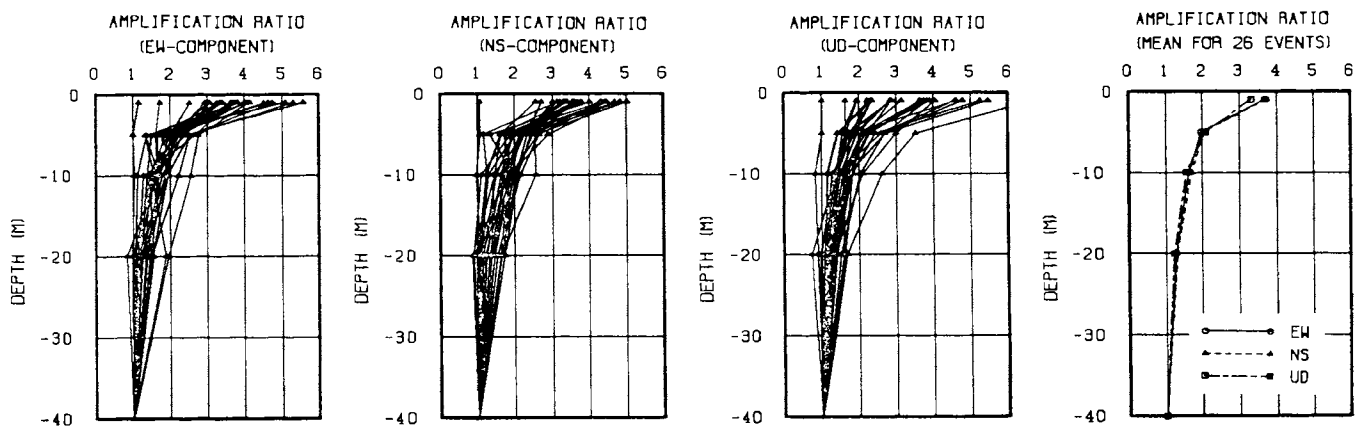
Fig. 4 Amplification Ratios of Peak Ground Acceleration at Borehole C0

acceleration was considerably amplified by this top soft layer. But for peak ground displacement, the top soft layer does not show apparent amplification. From GL -40m to GL -1m, the amplification of peak displacement could hardly be found although figures are not shown here.

Although the amplification ratios show some difference among events, the peak acceleration is amplified when the seismic wave propagates upward. One exception showing no amplification for all three components was found among the events and was identified as the 1984 Naganoken-Seibu earthquake (#5 in Fig. 3). The surface wave was found to be dominant in this event (Turker et al., 1990). It was also noticed at the Chiba array site that the amplification ratio of peak acceleration for the vertical component shows a close value with the horizontal components.

The average of the amplification ratios was calculated for 26 events excluding the exception as shown in Fig. 4. While the amplification ratio differed for the two horizontal components for individual events, the average have almost the same value for all the depths. The average amplification ratio of peak acceleration at GL -1m showed a value of 3.7 and that at GL -5m a value of 2. This means that the peak acceleration at GL -5m decreased to about half of that at the ground surface. The amplification ratio of peak acceleration was also calculated for the other 10 boreholes shown in Fig. 1. Although the amplification ratios show some differences among the boreholes for individual events, their average values are very close for all the three components.

Amplification of Recorded Motion

Soil amplification characteristics were investigated in this part with the aid of Fourier spectrum ratio, A(f), and coherence function, $coh^2(f)$:

$$A(f) = \left(\frac{S_{yy}(f)}{S_{xx}(f)}\right)^{\frac{1}{2}} \quad ...(1) \qquad coh^2(f) = \frac{|S_{xy}(f)|^2}{S_{xx}(f)\, S_{yy}(f)} \quad ...(2)$$

where $S_{xx}(f)$ and $S_{yy}(f)$ are the power spectra of the input

and output motions respectively and $S_{xy}(f)$ is the cross spectrum. The smoothing technique was employed with a Parzen window of 0.4Hz bandwidth to estimate these spectra from a pair of ground accelerations while the ensemble average for 16 events was used to estimate these spectra statistically. These 16 events were selected from the 27 events which have a large peak value and long duration. In the case of the ensemble average, the power spectra of output motions was normalized by the area of $S_{xx}(f)$ for each event due to the large power difference of each event.

The ensemble Fourier spectrum ratio, coherence function and phase lag calculated for the 16 events are shown in Fig. 5 for the records at GL -1 and GL -40m in borehole C0. Those were also calculated for the 16 individual events by the smoothing procedure and those for the 1985 Ibaragiken-Nanbu earthquake (#9 in Fig. 3: IEQK = 8519) are shown in Fig. 5 by a dashed line. While the results of the ensemble average are not smooth enough due to the limited number of samples, peaks can be clearly seen in them. The smoothed Fourier spectrum ratio, coherence function and phase lag are mostly close to those from the ensemble but some of the events show some difference. The Fourier spectra and coherence functions from the ensemble average for the two horizontal components are very close each other but those of the vertical component are different from them. The difference is caused by a different wave type because it is often the case that the S wave is dominant in the horizontal motion and the P wave is dominant in the vertical motion. It is noticed that the smoothing procedure generally gives a satisfactory estimation but the difference between two horizontal components remains.

The coherence function was generally high between the ground motions recorded at GL -1m and GL -40m except for some drops at certain frequencies. The drop of the coherence function was found to just occur at the natural frequencies. Both that from ensemble average and that by smoothing show the same phenomenon. The drop of the coherence function is caused by the rapid change of phase
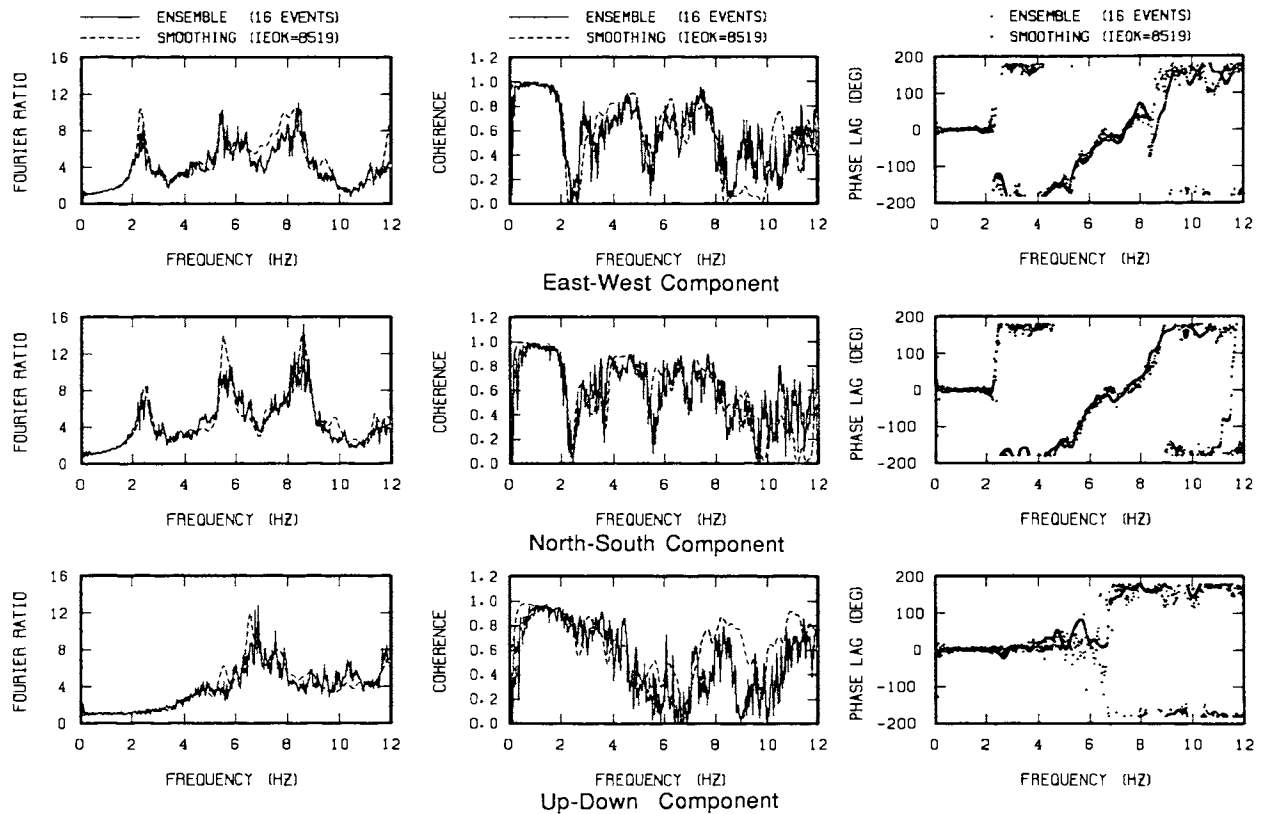
Fig. 5 Fourier Spectrum Ratios and Coherence Functions by Ensemble and Smoothing (C001/C040)

lag between input and output motions. It is known that the phase lag changes rapidly around the natural frequency especially when damping is small. Therefore, the phase lag at natural frequency is very sensitive to a small variation in the stiffness of the system and a slight randomness in soil properties. Actually the phase lag around the natural frequencies obtained from the 16 events were highly scattered. It is common for a complex number to take the average of the real part and imaginary part respectively. As $S_{xy}(f)$ is obtained by averaging, the amplitude of $S_{xy}(f)$ become very small due to the effect of the scattered phase lag. While $S_{xy}(f)$ is obtained by smoothing, the rapid change of phase lag around the natural frequencies causes the similar effect as frequency window crossing the natural frequencies. Thus, the high value of coherence function out of the natural frequencies together with the drop around the natural frequencies implies that the seismic wave propagates vertically.

The transfer function, H(f), was also calculated from the ensemble average and from individual events by smoothing.

$$H(f) = \frac{S_{xy}(f)}{S_{xx}(f)} \qquad \qquad ......(3)$$

The amplitude of the transfer function is very close to the Fourier spectrum ratio in shape but often shows a drop around the natural frequencies. The drop of the transfer

function is due to the drop of coherence function because o the relationship between the transfer function, Fourie spectrum ratio and coherence function as follows.

$$| H(f) | = \sqrt{coh^2(f)} \; A(f) \qquad ......(4)$$

Although in most cases, Eq. 4 gives a good estimation o the amplitude of the transfer function (Bendat and Piersol 1971), it should be pointed out here that the amplitude o the transfer function around natural frequencies is much smaller than that of the actual amplification of the site One method to calculate the transfer function with eliminating the effect of the rapid change of phase lag ha: been discussed (Lu et al., 1990).

The ensemble power spectra and ensemble transfer functions were calculated for boreholes C0 and P5. Figure 6 shows the power spectra at GL -1m and the transfer function between GL -1m and GL -20m for the twc boreholes. While the transfer function between GL -1m and GL -40m and that between GL -1m and GL -10m at borehole P5 are similar to those at borehole C0, the transfer function between GL -1m and GL -20m is quite different for the two boreholes. The transfer function ot borehole C0 for GL -1m to GL -20m clearly shows peaks while that of borehole P5 does not. Consequently, the power spectra at GL -1m differs for the two boreholes. From Fig. 2, it is noticed that there is a stiff intermediate

ayer from about 12.5m to 15m in the soft layers. This stiff ayer may cause the difference of the transfer function and ·ower spectra between the two boreholes.

ʾOMPARISON OF MICROTREMOR WITH ꞮARTHQUAKE GROUND MOTION

ᴠleasurement of Microtremor
ᴠlicrotremor was measured at the ground surface of the Ɜhiba Experiment Station corresponding to the location of .1 boreholes shown in Fig. 1. Pickups used in the

Fig. 6 Ensemble Power Spectra (GL -1m) and Transfer Functions (GL-1/GL-20) for 16 events

measurement are velocity type ones with a natural frequency of 2 seconds and a viscous damping ratio of 0.64. Because of the limited number of pickups, they were measured 6 times with each time measuring 2 to 4 points. The observation was done during 10:30pm to 4:30am on a fine day with a weak wind. The velocity of microtremor was recorded continually for more than 5 minutes at each point for the east-west, north-south and up-down components.

The comparison of the properties of microtremor with those of the earthquake records was conducted in velocity. By integrating the recorded earthquake acceleration, the velocity of the earthquake ground motion was obtained . Figure 7 shows one example of the time histories of microtremor and earthquake for the three components.

Comparison of Power Spectrum
The power spectra were calculated for the microtremor records by applying the smoothing process with a Parzen window of 0.4Hz bandwidth. In the calculation of the power spectrum, the earthquake ground motion records of 40 seconds was employed and 1 minute of microtremor selected from the original 5 minutes was used. The power spectra for the three components of microtremor recorded at borehole P1 are shown in Fig. 8(a) and those calculated from the records of the 1985 Ibaragiken-Nanbu earthquake are shown in Fig. 8(b).

The power spectra of the three components are rather close both in shape and in amplitude for microtremor. In the case of the earthquake records, however, the power spectrum of the vertical component is different from those of the horizontal components with a smaller amplitude and different peaks. The difference appears at frequencies less than 1Hz between the two horizontal components for this event. However, it does not occur for some other events. It is noticed that the power of the earthquake ground motion
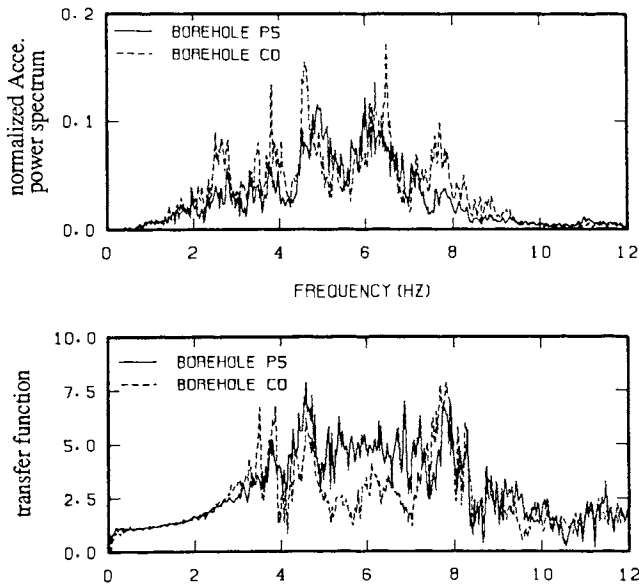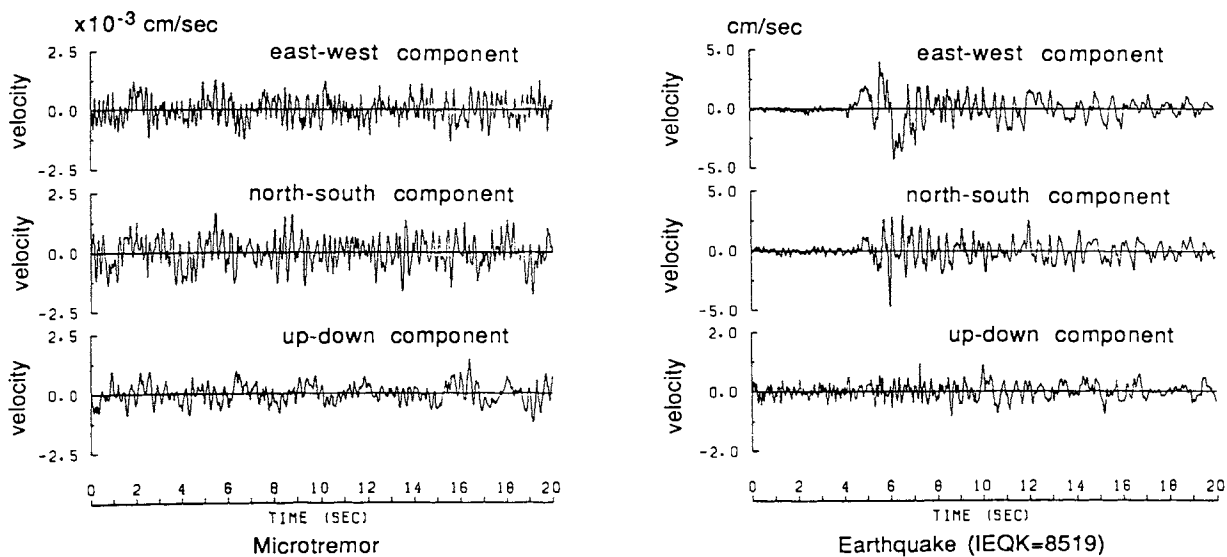
Fig. 7 Time Histories of Velocity for Microtremor and Earthquake (IEQK=8519) at Borehole P1

comes mainly from the S wave in the horizontal components and from the P wave in the vertical component. Therefore, the power spectra of the vertical component and horizontal components reflect the different vibration properties of the site. In the case of microtremor, there is no significant difference among the three components. Thus, the vertical component of microtremor gives the same information as that of the horizontal components.

The power spectra were calculated for the 9 strong events included in the Chiba Array Database. Three of them (#9: IEQK=8519, #16: IEQK=8722 and #27: IEQK=8904 in Fig. 3) are shown in Fig. 9 together with that of microtremor for the NS-component at borehole P1. In this

figure, the power spectra were normalized by their ow area in order to make the comparison easier. In the case r microtremor, the first peak appeared at about 0.5Hz an the second peak appeared at a frequency of about 2.5Hz an some other peaks at frequencies higher than 4Hz. Th power spectra of some earthquakes show a peak aroun 0.5Hz and some do not show a peak. The power spectra c all the 9 earthquakes show a peak around 2.5Hz and 6 c them are dominant around this frequency. The agreemer of the peak around 2.5Hz between microtremor an earthquake can be observed very well. For the peaks a frequencies higher than 4Hz, a consistent agreement cannc be found. Thus, it is difficult to comment on these peaks.

The microtremor was measured at the 11 points and th power spectra were calculated. At the same time, the powe spectra at the same points for the earthquake (IEQK 8519) were also computed and are shown in Fig. 10. Th power spectra of the 11 points were rather close for th earthquake records in the whole frequency range. In th case of microtremor, a larger difference was found. I should be noted that the difference for a single event onl included the effect of soil condition while the difference ir microtremor further included the effect of measuremen time. The peak around 2.5Hz generally agreed wel between microtremor and earthquake records.

The first two peaks of microtremor were furthe investigated in detail. With the aid of a frequency filter the motion of microtremor was selected in a frequenc range of 0.4 to 0.8Hz. The apparent wave velocity of th

cm²/sec

(a) Microtremor

cm²/sec
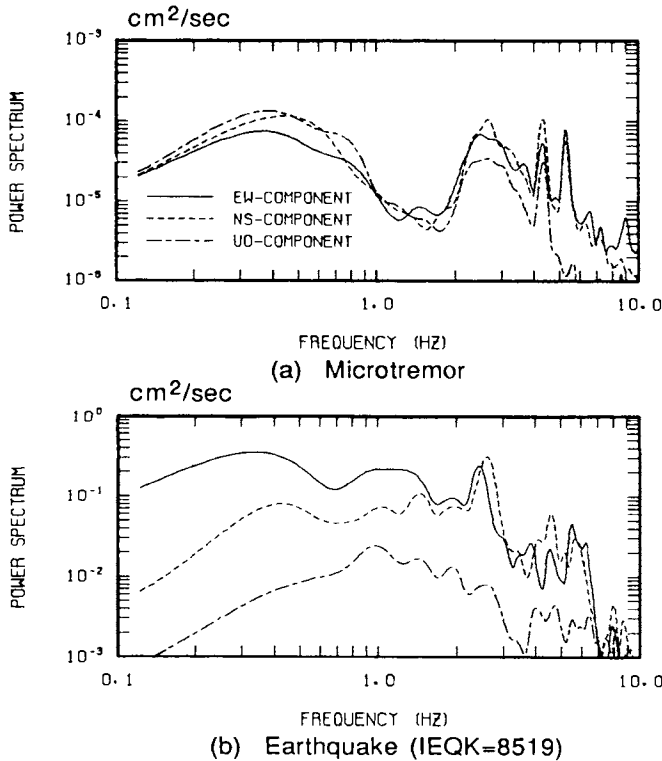
(b) Earthquake (IEQK=8519)

Fig. 8 Power Spectra of Three Ground Motion
Components at the Location of Borehole P1

Fig. 9 Power Spectra of NS-component for Microtremor
and Earthquake Events at the Location of Borehole P1

cm²/sec

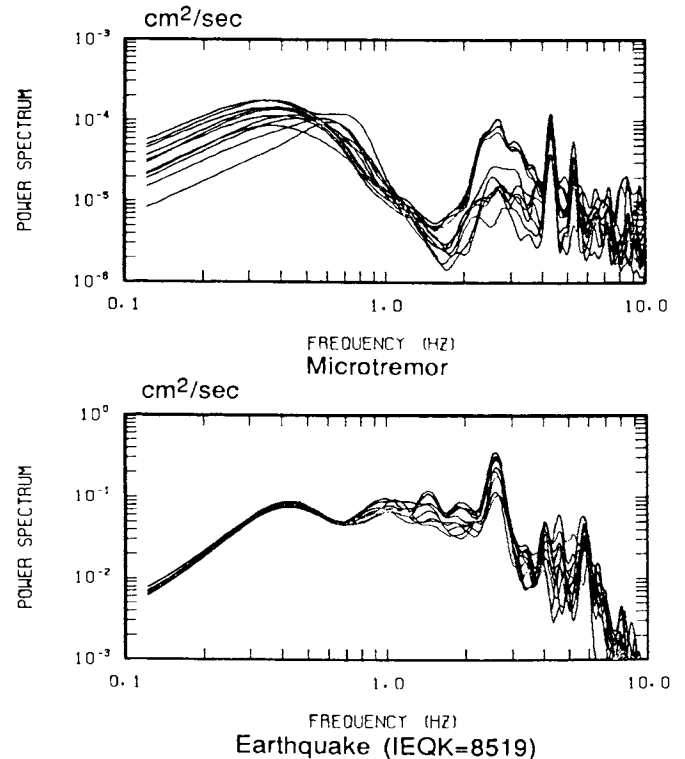Microtremor

cm²/sec

Earthquake (IEQK=8519)

Fig. 10 Power Spectra of NS-component for 11 Locations

Table 2 Soil Structure Model for the Chiba Station

DEPTH (km)	V_p (m/s)	V_s (m/s)	ρ (gr/cm³)	models & sublayers		
				M1	M2	M3
0.005	320	140	1.15			1
0.010	550	320	1.50	1	1	1
0.015	550	320	1.95			1
0.024	1670	320	1.95	1	1	1
0.040	1670	420	2.00			1
0.500	2100	500	2.10	8	8	8
1.000	2150	820	2.20	5	4	8
2.500	2550	1525	2.40	5	3	3
10.000	5600	3000	2.60	3	3	
35.000	6700	3900	2.70	3		
90.000	7500	4300	2.90	3		

model 1 0.1 < k < 1.0 $k = \dfrac{\omega}{c}$

model 2 1.1 < k < 7.0   k = wave number(rad/m)

model 3 8.0 < k < 100.   ω = circular freq.(rad/s)
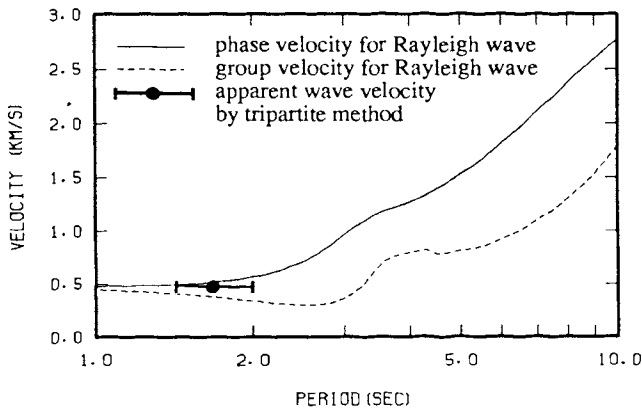
c = apparent velocity(m/s)

Fig. 11 Comparison of Theoretical Dispersion Curve and Measured Apparent Velocity by Microtremor

filtered wave was calculated by the tripartite method using the records for points C0, P5 and P6. It gives the result of 460m/s. By applying the same procedure to the microtremor at points P1, P2 and P4 with a frequency window of 2.2 to 3.2Hz which covers the frequency range of the second peak, an apparent velocity of 2960m/s was obtained. The dispersion curve for the Rayleigh wave can be calculated (Lysmer, 1970) theoretically by modeling the site as a horizontal layer. According to the site model of the Chiba Experiment Station shown in Table 2 (Turker et al., 1990), the dispersion curve for the Rayleigh wave (the fundamental mode) was obtained as shown in Fig. 11. It was found from the figure that the apparent wave velocity of the microtremor between 0.4 to 0.8Hz calculated from the tripartite method is very close to the phase velocity of the theoretical dispersion curve. Thus, the first peak of microtremor may be due to the Rayleigh wave.

Since the apparent wave velocity of the microtremor corresponding to the second peak is large, the wave between 2.2 to 3.2Hz may have been a body wave coming

from the deeper layers. Thus, the coincidence of the peak of power spectra around the 2.5Hz between the microtremor and earthquake ground motion is meaningful and indicates that the microtremor is affected by the local site condition and this site effect is similar to that under earthquake excitation.

Comparison of Spatial Correlation Characteristics

The spatial coherence of the microtremor was also investigated and compared with that of the earthquake ground motion (IEQK = 8519). The coherence function between boreholes P1 and P3, which are separated by a distance of 30m, and that for boreholes C0 and P5 which are at a distance of 124m, were calculated as shown in Fig. 12. The coherence function for the microtremor decreases as the frequency increases and as separation distance increases. The coherence function for the earthquake shows the same tendency. However, the coherence function for the microtremor decrease more rapidly than that for the earthquake as the separation distance and frequency increase. The coherence function for the microtremor is only high in the low frequency range which corresponds to the coherent wave propagation through the site. For the higher frequency, the microtremor becomes spatially incoherent which indicates different vibration sources and/or random incident angles for different locations. In the case of earthquake, however, the higher frequency contents also consist of coherently travelling waves.

CONCLUSIONS

Soil amplification characteristics of earthquake ground motion were investigated based on the Chiba Array observation records. The amplification of peak acceleration mostly occurred at a few meters below the ground surface, which is considered to be caused by the top soft layer. Although there were differences among events and among boreholes, their average was very close for the two horizontal components and rather large amplification was also observed for the UD-component.

The ensemble Fourier spectrum ratio and coherence function were calculated between the ground motions of several depths. The amplification of the Fourier spectrum ratio and the drop of the coherence function were clearly seen at natural frequencies, which means that the seismic wave mainly propagates vertically. The Fourier spectrum ratio and coherence function were also obtained using the smoothing procedure for each event and were compared with those of the ensemble. The smoothing procedure generally gives a satisfactory estimation but the difference between each event and two horizontal components remains.

Microtremor was measured at 11 points corresponding to the location of the surface accelerometers. The peak appeared around 0.5Hz in the power spectra of microtremor and may be due to the Rayleigh wave and the peak around 2.5Hz may probably be caused by the body

| MICROTREMOR | | |
| EARTHQUAKE | | |

EW NS UD

Borehole P1 and Borehole P3 (d=30m)

EW NS UD
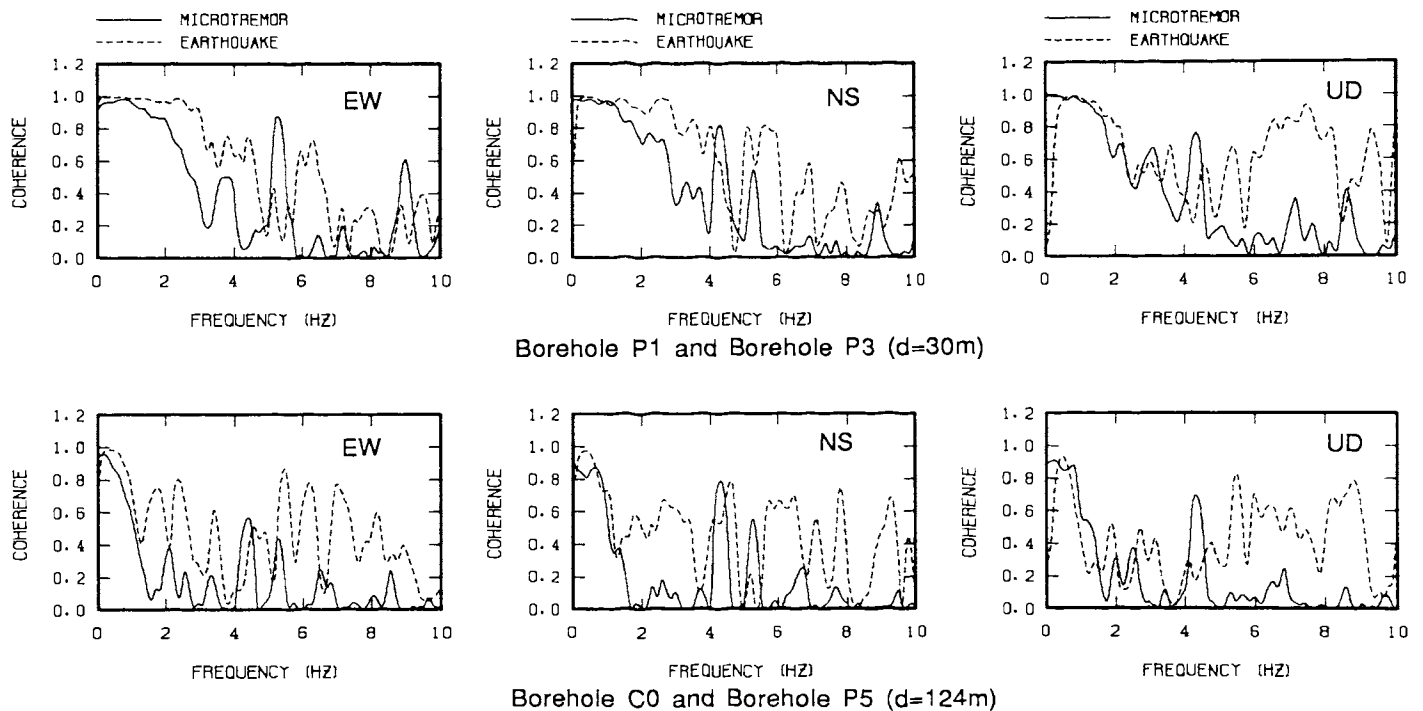
Borehole C0 and Borehole P5 (d=124m)

Fig. 12 Coherence Functions for Microtremor and Earthquake Ground Motion (IEQK=8519)

wave propagating upward. The power spectra of microtremor were compared with those of earthquake ground motion for different points and for different events. The peak around 2.5Hz coincided very well between the microtremor and earthquake records. This coincidence indicates that the same local site effect was involved in the microtremor and earthquake ground motion.

ACKNOWLEDGEMENTS

REFERENCES

Bendat, J. and Piersol, A.: "Random data: analysis and measurement procedures," John Wiley & sons, 1971.

Benuska, L. et al.: "Loma Prieta earthquake reconnaissance report," Earthquake Spectra, Supplement to Vol. 6, 1990.

Bertero, V.: "The 19 September 1985 Mexico earthquake: building behavior," UCB/EERC-86/08, 1986.

Kanai, K. and Tanaka, T.: "On Microtremors, VIII," Bulletin of the Earthquake Research Institute, Vol.39, pp. 97-114, 1961.

Katayama, T. and Sato, N.: "Ground strain measurement by a very densely located seismometer array," Proc. of 6th Japan Earthquake Engineering Symposium,

pp. 241-248, 1982.

Lu, L., Yamazaki, F. and Katayama, T.: "Estimation of frequency response function from earthquake ground motion," Proc. of 45th Annual Meeting, JSCE, 1990.

Lysmer, J.: "Lumped mass method for Rayleigh waves," BSSA, Vol. 60, No. 1, 1970.

Nagata, S., Katayama, T., Yamazaki, F., Lu, L. and Turker, T.: "A dense seismograph array in Chiba, Japan and its strong motion database," Proc. of 4th U.S. National Conference on Earthquake Engineering, Vol. 1, pp. 357-366, 1990.

Sherif, M.: "Microzonation with respect to site amplification and soil liquefaction," Proc. of Joint US-PRC Microzonation Workshop, Harbin, 2-1-64, 1981.

Turker, T., Yamazaki, F. and Katayama, T.: "Analysis of seismic wave propagation based on the Chiba array database," Proc. of 8th Japan Earthquake Engineering Symposium, 1990.